

한국표면공학회지  
Journal of the Korean Institute of Surface Engineering  
Vol. 34, No. 5, Oct. 2001  
<연구논문>

## Growth and characterization of BON thin films prepared by low frequency RF plasma enhanced MOCVD method

G. C. Chen, D. -C. Lim, S. -B. Lee, B. Y. Hong, Y. J. Kim, and J. -H. Boo

*Center for Advanced Plasma Surface Technology, Sung Kyun Kwan University,  
Suwon, 447-740, Korea*

### Abstract

It was first time that low frequency R. F. derived plasma enhanced MOCVD with trimethylborate precursor was used to fabricate a new ternary compound  $\text{BO}_x\text{N}_y$ . The formation of BON molecule was resulted from nitrogen nitrifying B-O, and forming the angular molecule structure proved by XPS and FT-IR results. The relationship between hardness and film thickness was studied. An thickness-independent hardness was found about 10 GPa. The empirical calculation of band-gap and UV test result showed that our deposited  $\text{BO}_x\text{N}_y$  thin film was semiconductor material with 3.4 eV of wide band gap. The electrical conductivity,  $4.8 \times 10^{-2} (\Omega \cdot \text{cm})^{-1}$  also confirmed that  $\text{BO}_x\text{N}_y$  has a semiconductor property. The roughness detected from the as-grown films showed that there was no serious bombarding effect due to anion in the plasma occurring in the RF frequency derived plasma.

### 1. Introduction

The materials, composed of boron (B) with other light elements such as nitrogen (N), carbon (C), oxygen (O), etc, are interesting, because of their excellent properties for superhardness<sup>1)</sup>, insulation<sup>2)</sup> and nonlinear optical behavior<sup>3)</sup>. Thus, they are attractive for wear protection<sup>4)</sup>, electronic device<sup>5)</sup> and wide band-gap optoelectrical device<sup>6)</sup> and laser device<sup>3)</sup>. Recently, the possibility on the existence of boron oxynitrogen (BON) compound has been proposed<sup>7)</sup>. However, there has no report on fabrication and property of this materials in detail yet. Radio frequency (R.F.) plasma enhanced metalorganic chemical vapor deposition

(MOCVD) has been successfully applied into the fabrication of oxide<sup>8)</sup>, nitride<sup>9)</sup> and boron-containing materials<sup>10)</sup>. The frequency was usually 13.56 MHz in these cases. High ratio of gas-phase molecule dissociation was expected<sup>11)</sup> by using such a high frequency that may be resulted in the multi-deposit fabrication of multi-elements compounds. To avoid this disadvantage, a deposition process with low frequency is highly desirable. In this paper, therefore, we reported the fabrication of BON thin films by low frequency (100 kHz) derived plasma enhanced MOCVD using an organoborate precursor. The composition and surface morphology of BON films were determined by x-ray photoelectron spectroscopy (XPS), SEM, and

Fourier transform infrared (FT-IR) spectroscopy. The hardness, surface roughness and optical band-edge absorption property were also presented.

## 2. Experimental

The procedure of BON fabrication was done in a set of parallel plate electrode discharge deposition system. The plasma was derived by R.F. with 100 kHz frequency and 500 W power. The plasma source gases were Ar/N<sub>2</sub>/H<sub>2</sub>, in which the flux was 200 sccm, 20 sccm, respectively. The trimethylborate, (OCH<sub>3</sub>)<sub>3</sub>B (TMB), was used as boron and oxygen source. It was introduced into the reactive zone of deposition chamber by a gas distribution ring which had pine-holes on it. The flux was 2.2 sccm without carrier gas. The working pressure 2 Torr in the chamber. The substrates

applied in this study were one-side polished single crystalline silicon wafer with (001) crystal surface and micro cover glass. Before they were installed on the substrate heater in the deposition chamber, they underwent degreasing and drying in vacuum. The substrate temperature measured by thermocouple and controlled by a commercial temperature controlling system was kept at 500 °C during deposition. The longest deposition time was 5 hours.

## 3. Results and Discussion

Figure 1 is the binding energies of B<sub>1s</sub>(a), O<sub>1s</sub>(b), N<sub>1s</sub>(c) and C<sub>1s</sub>(d) of an as-grown BON film obtained by high resolution XPS. The values are as similar as those in ref.7, where B(O,N) was declared. Since the binding energy of N<sub>1s</sub> is higher

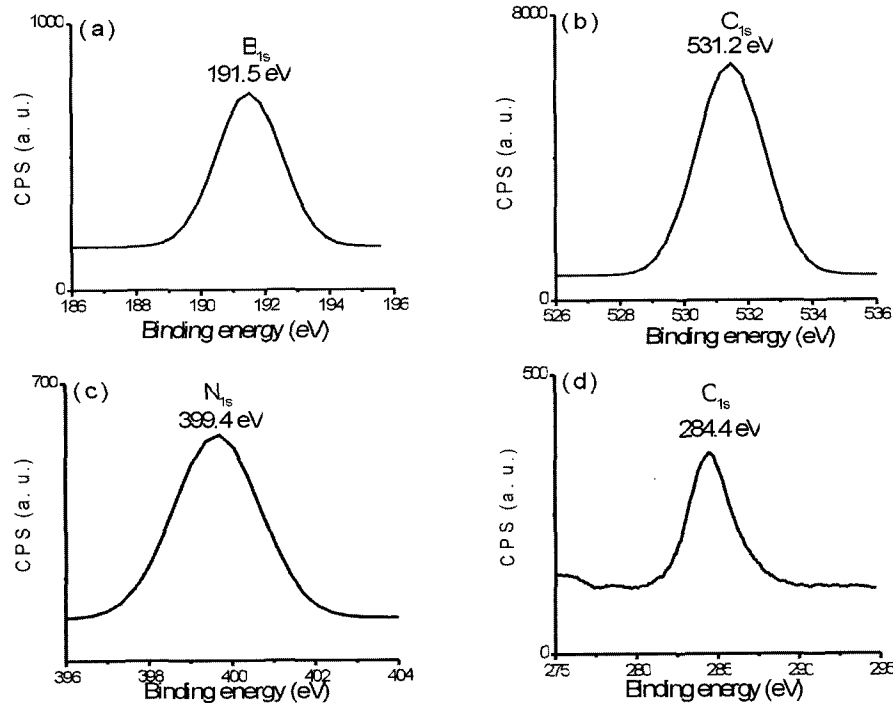


Fig 1 High resolution x-ray photoelectron spectra of a BON thin film grown on Si (100) substrate at 500 °C for 4hrs : (a) B<sub>1s</sub>, (b) O<sub>1s</sub>, (c) N<sub>1s</sub> and (d) C<sub>1s</sub>.

than 398.1 eV, attributing to direct bond between B and N atoms<sup>12)</sup>, N is more closely bonded to O rather than to B. On the other hand, the binding energy of O<sub>1s</sub> and B<sub>1s</sub> are also smaller than 533.24 eV and 193.70 eV respectively. That means there is no B<sub>2</sub>O<sub>3</sub> structure in the films<sup>13)</sup>. Therefore, the molecule of B(O,N) seems to be reasonable as BON. The XP survey spectrum (not shown) also shows that the content of carbon is reduced obviously after the Ar ion sputtering. As the sputtering depth is less than 3 nm, the carbon is the absorbance of the BON surface. The atomic composition of as-grown films after sputtering were determined as: 30.6% B, 42.1% O, 27.2% N. The stoichiometric formula were thus determined as BO<sub>1.4</sub>N<sub>0.9</sub>. The compositions of all as-grown films are also confirmed with RBS.

Fig. 2a is the FT-IR result obtained from the BON film grown on Si (100) substrate at 500 °C for 4hrs. It shows that there is abroad and strong peak at 1580-1270 cm<sup>-1</sup>. The peak occurring at this range was regarded as graphite carbon structure<sup>14)</sup>, B-O<sup>15)</sup> and B-N<sup>16)</sup>, respectively. Based on the analysis of binding energies in Figs. 1 (a) ~ 1 (c), our film can have the B-O-N̄ bond. So, this peak can be regarded as B-O-N feature vibration in IR spectra. Then the bond type in the films is very similar to B-O-N. Notice the peak at 1351 cm<sup>-1</sup>. It is well known that h-BN has two vibration frequencies at 1390 and 750 cm<sup>-1</sup><sup>16)</sup>. In our case, B may not directly be bonded with N as mentioned above. One can imagine that the interaction between B and N is weaker than that in BN. That means the smaller k value in the formula of

$$\nu = \frac{A}{2\pi} \sqrt{\frac{k}{\mu}} \quad (\nu \text{ is vibration frequency in IR, } A \text{ is proportional constant, } k \text{ is force constant, } \mu \text{ is}$$

reduced mass). So, the vibration due to this interaction will occur at lower energy range than that in the BN for IR spectra. thus, we regard that the peak at 1351 cm<sup>-1</sup> shows the interaction between B and N with weak force constant compared to h-BN. If BON is linear structure, the distance will be 3.85 Å (R<sub>oxygen</sub>=0.61 Å) which is about 3 times as long as the BN bond length according the data in ref.17. Such a long distance is impossible for B and N to form an enough strong interaction, and can not be detected by IR. So, we concluded that the atoms of B, O, N in the films prefer to angular structure rather than linear one. The peaks occurring at the range of 1100-600 cm<sup>-1</sup> in Fig. 2a are thus due to B-O-Si bridge at (930-915, 675-600 cm<sup>-1</sup>) and Si-O (1100, 840-790 cm<sup>-1</sup>)<sup>18)</sup>. From the XPS and IR results, it can be seen that the bond between B and O in BON is "inherited" from the precursor. The formation of BON bond is therefore the result of activated nitrogen nitrifying the B-O radical. The maintaining of B-O bond in the BO<sub>x</sub>N<sub>y</sub> films can be ascribed to the low frequency derived plasma deposition condition. This indicates that low frequency derived plasma is one of the available methods for material fabrication to utilize the former bond existence in the precursor.

The band-edge absorption of the film grown on a glass substrate was detected by ultraviolet (UV)/visible absorption spectra, shown in the Fig. 2b. The film has not high transmittance (about 50%) in the infrared, through the visible and into the UV, where it drops sharply due to the band edge of the material. With the almost the straight-line interception at about 360 nm wavelength, a band-gap of 3.4 eV is deduced. The electrical conductivity of the film was also measured by 4-points

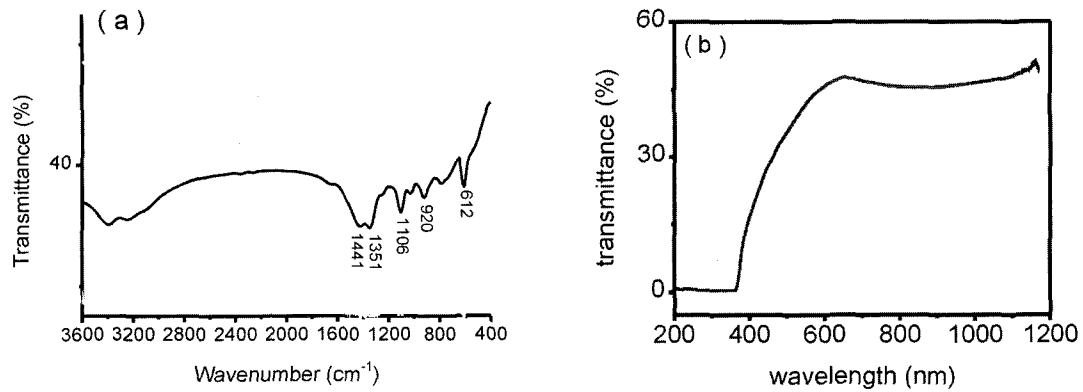


Fig. 2 Typical FT-IR (a) and UV-visible (b) spectra of  $\text{BO}_x\text{N}_y$  thin films grown on Si (a) and glass (b) substrates at 500 °C for 4hrs.

probe method. The conductivity was  $4.8 \times 10^{-2} (\Omega \cdot \text{cm})^{-1}$ .

These results show the wide band gap feature of the gained films, suggesting a semiconductor property. If assuming the full p shell for both O and N in  $\text{O}_x\text{N}_y$  radical, the electronegativity of radical  $\text{O}_{1.4}\text{N}_{0.9}$  is 2.6 according to the calculation of group electronegativity  $X = \frac{Ng}{\sum(\eta/\chi)}$  ( $N_g$  is the number of atoms in group formula;  $\eta$  is the number of a particular element in the group;  $\chi$  is the electronegativity of the particular element.)<sup>19</sup>. In terms of the empirical relationship<sup>20</sup> between the band gap and the electronegativity, the band gap of  $\text{BO}_x\text{N}_y$  is very close to 3.6 eV. Our result is little small than the calculated one. This may be ascribed to carbon contents in the deposited films. Usually, carbon can reduce the transmittance of UV. In our case, the UV detection was done in the open air. The film was not clean by ion sputter, signifying that some parts of carbon was incorporated by precursor itself during deposition. The carbon in/on the film surfaces made low transmittance near the band-edge. So, the measurement value tends to become small. This result suggests

that the band gap of  $\text{BO}_x\text{N}_y$  can be tailored from insulation to semiconductor by the changes of the nitrogen and/or oxygen of  $\text{BO}_x\text{N}_y$  in UV protection<sup>21</sup>.

The microhardness test for the as-grown films on Si substrate was carried out by using Knoop indenter under the following condition; 25 g load, 10 sec load time, 5 sec held time, 5 sec unload time. The dependence of hardness and thickness is shown in Fig. 3. When the thickness of films are less than 1 micron (in zone I), the hardness decreases with the increase of thickness. More than 1 micron, the hardness firstly increases with the

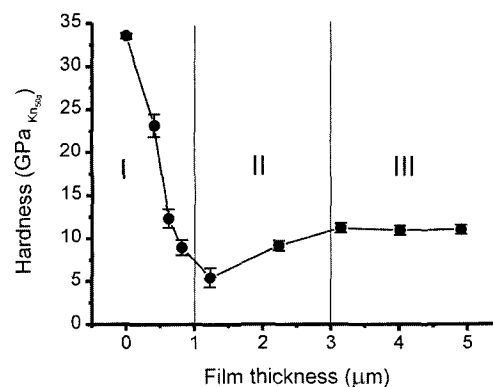


Fig 3 Dependence of microhardness and film thickness.

thickness (in zone II), then arrives at a thickness-independent value, which is about 10 GPa (in zone III). This value is comparable with the one obtained from low carbon content BNCO film reported previously<sup>22)</sup>. As the hardness of BON film is not high, the change of hardness in zone I may be ascribed to the reduction of substrate effect<sup>23)</sup>.

The characteristic of SEM morphologies (see Fig. 4) at different thickness zones are also investigated. The surfaces of the films show very smooth feature for the thickness less than 1 micron (zone I). In the region between 1 and 3 micron (zone II), the films are non-continuous. Thicker than 3 microns (zone III), the films become successive. So, the minimum hardness in the zone II may lie in the non-perfect film structure. As the film structure is stable in the zone III, the hardness value is no-changed. That is why the non-continuous film morphology observed by SEM. As the plasma condition were the same in these three zones, the change of roughness is due to the film structure rather than the plasma condition. In fact, the roughness, except zone II, is small compared to the result gained by ECR method in AlN

film surface<sup>11)</sup>. This means that there is little ion bombarding effect in our experimental condition. It indicate that low frequency derived plasma can also be used in semiconductor material fabrication by properly designing the reactive chamber. On the other hand, the change of roughness is in the range of nanometer scale. This means that the roughness changes can not influence to the hardness very much under our measurement condition. So, the change of harness is strongly or mainly related to the film structure rather than roughness.

#### 4. Conclusions

A new ternary elements compound  $\text{BO}_x\text{N}_y$  was fabricated by 100 kHz frequency derived plasma enhanced MOCVD method with trimethylborate precursor. The formation of  $\text{BO}_x\text{N}_y$  was the result of activated nitrogen nitrifying B-O radicals, and formed angular molecular structure. The stoichiometry of this material was determined as  $\text{BO}_{1.4}\text{N}_{0.9}$ . The experimental results showed that it was a semiconductor with 3.4 eV band gap and  $4.8 \times 10^{-2} (\Omega \cdot \text{cm})^{-1}$  electrical conductivity as well as

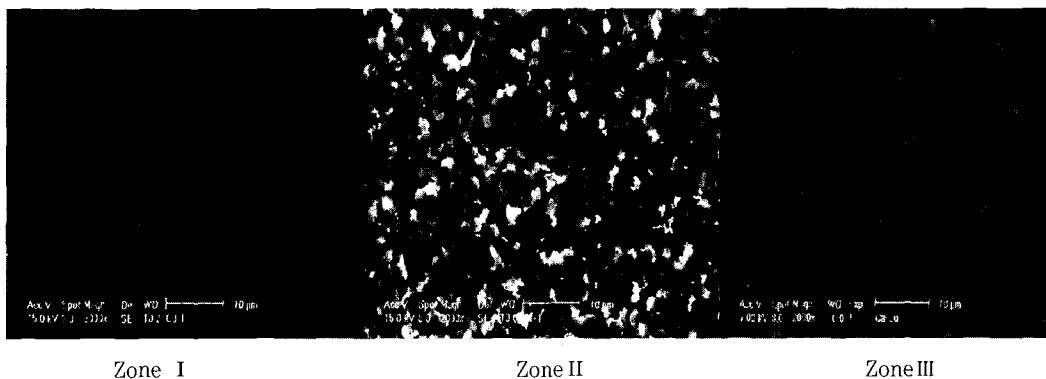


Fig. 4. SEM images of the BON films in different thickness zones shown in figure 3: (a) in zone I; (b) in zone II; (c) in zone III.

10 GPa hardness. The fabrication of  $\text{BO}_x\text{N}_y$  also showed that low frequency derived plasma deposition condition was suit for material fabrication to utilize the bond occurring in precursor.

### Acknowledgements

One of the author, G. C. Chen, would like to thank for support of BK21 project. Supports of this research by the Korea Research Foundation through BSRI project (2000-015-DP0195) and by the Center for Advanced Plasma Surface Technology of Sungkyunkwan University are also gratefully acknowledged.

### References

1. T. Lundstrom and Y. G. Andreev, *Mater. Sci. & Eng. A* 209, 16 (1996) .
2. R. C. DeVries, in "Cubic Boron Nitride: Handbook of Properties", General Electric Rep. No. 72CRD178, p. 72.
3. D. Xue and S. Zhang, *Appl. Phys. A* 65, 451 (1997) .
4. J. Tian, L. Xia, X. Ma, Y. Sun, E. S. Byon, S. H. Lee, and S. R. Lee, *Thin Solid Films*, 355/356, 229 (1999) .
5. S. P. S. Arya and A. D'aMico, *Thin Solid Films*, 157, 267 (1988) .
6. J. H. Boo, C. Rohr, and W. Ho, *J. Cryst. Growth*, 189/190, 439 (1998) .
7. S. Sahu, S. Kavecky, L. Illesova, J. Madejova, I. Bertoti, and J. Szepvolgyi, *J. Eurp. Cerem. Soci.*, 18, 1037 (1998) .
8. K. H. A. Bogart, N. F. Dalleska, G. R. Bogart, E. R. Fisher, *J. Vacu. Sci. & Technol.*, A 13, 476 (1995) .
9. M. R. Hilton, L. R. Narasimhan, S. Nakamura, M. Salmeron, and G. A. Somorjal, *Thin Solid Films*, 139, 247 (1986) .
10. H. Miyamoto, M. Hirose, and Y. Osaka, *Jpn. J. Appl. Phys.* 22, L216 (1983) .
11. C. R. Abernathy, J. D. Mackenzie, and S. M. Donovan, *J. Cryst. Growth*, 178, 74 (1997) .
12. K. S. Park, D. Y. Lee, K. J. Kim, and D. W. Moon, *Appl. Phys. Lett.*, 70, 315 (1997) .
13. G. D. Khattak, M. A. Salim, L. E. Wenger, and A. H. Gilani, *J. Non-crystalline Solids*, 244, 128 (1999) .
14. X. A. Zhao, C. W. Ong, Y. C. Tsang, Y. Wong, P. W. Chan, and C. L. Choy, *Appl. Phys. Lett.*, 66, 2652 (1995) .
15. W. Zimmerman, A. M. Murphy, and C. Feldman, *Appl. Phys. Lett.*, 10, 71 (1967) .
16. R. F. Davis, M. J. Paisley, Z. Sitar, D. J. Kester, K. S. Ailey, K. Linthicum, L. B. Rowland, S. Tanaka, and R. S. Kern, *J. Cryst. Growth*, 178, 87 (1997) .
17. S. Su, *J. Molecular Structure*, 430, 137 (1998) .
18. G. D. Soraru, N. Dallabona, C. Gervais, and F. Babonneau, *Chem. Mater.*, 11, 910 (1999) .
19. J. E. Huheey, E. A. Keiter, and R. L. Keiter, "Inorganic Chemistry---Principles of structures and reactivity", (Harper Collins College Publishers. 1993) , p. 274.
20. S. G. Bratsch, *J. Chem. Edu.*, 62, 101 (1985) .
21. T. Masui, M. Yamamoto, T. Sakata, H. Mori, and G.Y. Adachi, *J. Mater. Chem.*, 10, 353 (2000) .
22. C. W. Ong, K. F. Chen, X. A. Zhao, and C. L. Choy, *Surf. & Coat. Technol.*, 115, 145 (1999) .
23. G. M. Pharr and W. C. Oliver, *MRS Bulletin*, 17, 28 (1992) .